JJMIE

Volume 19, Number 3, Sep. 2025
ISSN 1995-6665
Pages 491– 499
https://doi.org/10.59038/jjmie/190302
Editor-in-Chief: Prof. Ali M. Jawarneh

Jordan Journal of Mechanical and Industrial Engineering

Electrical and Mechanical Behavior of Chromium Disilicide Thin Films on Polyethylene Terephthalate under Tensile Strain

Atif Alkhazali[1*], Mohammad M. Hamasha[1], Sa'd Hamasha[2], Ibrahim Salem Alkhazali[3], Raghad Massadeh[4]

[1]Department of Industrial Engineering, Faculty of Engineering, The Hashemite University, Zarqa, 13133, Jordan
[2]Department of Systems Science and Industrial Engineering, State University of New York at Binghamton, Binghamton, NY 13902, USA (Visiting Professor, Department of Industrial Engineering, School of Applied Technical Sciences, German Jordanian University, Amman 11180,Jordan)
[3]Department of Mechanical and Industrial Engineering, Applied Science Private university, Amman, Jordan
[4]Department of Chemistry, Yarmouk University, Irbid, Jordan

Received 29 Mar 2025 Accepted 28 May 2025

Abstract

The present work is dedicated to the mechanical and electrical properties of CrSi2 thin films, deposited on PET substrates, in tensile strains, with a focus on issues concerning crack formation and increased strain-induced resistance degradation. CrSi2 is one of the most important semiconducting materials for flexible electronics, which has excellent thermal stability, high electrical conductivity, and remarkable robustness in various environmental conditions, making it an ideal candidate for wearable and stretchable applications. The tensile testing performed by mechanical testing along with in situ electrical resistance measurement provided quantification of PCER as a function of strain increase, while SEM carried out detailed observations of crack initiation and propagation for 100- and 200-nm $CrSi_2$ films to gain insight into their structural limits under applied mechanical stress. The thinner films of 100 nm presented faster crack formation and a rapid increase in resistance under smaller strains that caused earlier electrical failure, while in 200 nm films, higher thickness resulted in greater resistance to cracking and more variability in modes of failure. This study presents a novel investigation into the fracture mechanics of $CrSi_2$ thin films under tensile strain by providing a quantitative comparison between 100 nm and 200 nm thicknesses using in situ electrical resistance monitoring. The findings offer new insights into the critical role of film thickness in delaying crack initiation and mitigating electrical failure, thereby proposing a practical approach for optimizing the mechanical robustness and reliability of $CrSi_2$-based components in flexible electronic applications. The results strongly highlight the significant role of thickness in enhancing fracture resistance and maintaining electrical stability in $CrSi_2$ thin films. This finding provides valuable insightinto designing durable $CrSi_2$-based components in flexible electronic applications where reliability upon mechanical deformation is a prime consideration.

Keywords: Chromium Disilicide ($CrSi_2$) Thin Films; Flexible Electronics; Tensile Strain; Electrical Degradation; Crack Propagation; PET Substrates.

1. Introduction

Energy is the foundation of technological advancement and a key driver of modern civilization, with increasing demand pushing innovations across multiple sectors [1-5]. In particular, the transition toward sustainable, portable, and efficient energy solutions has heightened the importance of advanced electronic systems [6-8]. The demand for flexible electronics has risen considerably over the past few years due to their use in wearable devices, flexible displays, and stretchable sensors [9-21]. For the mentioned applications, electronic components that are functional and withstanding under various mechanical deformations during ordinary operation are required [22-28]. Flexible electronics have to withstand bending, stretching, and twisting—all of which impose significant electrical and mechanical demands on the used materials [29-32]. These demands create a challenge in preserving the structural integrity and electrical conductivity of the components under dynamic conditions.

Conductive thin films form the heart of flexible electronics, serving as critical conduction paths for electrical signals [33-40]. When deposited onto flexible substrates, these films have to continuously maintain electrical functionality even while being subjected to mechanical strains. The performance of these films under deformation relies heavily on their ability to resist stresses without significant deterioration in conductivity [41-43]. However, most conductive films are prone to cracking and delamination under either tensile or compressive stresses that disrupt the conductive network and lead to functional loss [44-45]. The challenge, therefore, is in the selection and engineering of such materials to handle such stresses with stability in electrical performance.

* Corresponding author e-mail: atif@hu.edu.jo.

An essential task in the development of reliable and long-lived flexible electronics is understanding the mechanical and electrical behaviors of thin films while in different states of strain [56]. By these studies, it is easy to see how materials will respond under different types and levels of strain. Factors that would eventually affect performance are identified, and by this token, develop a plan in which their resilience can be improved. Such knowledge will play the central role in design optimization for flexibility and fabrication, and it will ensure that, when subjected to real-world mechanical requirements, there is no significant loss of performance in the flexible electronic components. Consequently, the study of the strain-induced behavior of conductive thin films becomes a core activity in flexible electronics enhancement toward developing a new generation of innovative and adaptive electronic devices [47-48].

With the growing importance of flexible electronics in both wearable and foldable devices, there are numerous studies regarding the mechanical and electrical behavior of thin films on flexible substrates under stress. Indeed, research has shown that mechanical stress significantly affects the electrical performance differently for both TFTs and other flexible materials. For example, Gleskova et al., [49], commented that strain induces performance shifts in thin film transistors, notably in the creation of cracks beyond certain levels of strain. On the contrary, studies by Bensaid et al., [50], on organic TFTs, and Leterrier et al., 2010, on TFTs on steel and PI substrates show that different materials have different strain tolerance and different COS values. Gunda et al. [51] reviewed the mechanical characterization techniques of thin films that would help diagnose mechanisms of failure at the film-substrate interface in flexible device failures. Mohammed et al. [52] also worked out a-IGZO films deposited on PEN and PET substrates, showing that crack onset strains depend upon the substrate material, which, in turn, affects film resilience. Complementary to this, Han et al., [53] discussed AOS TFTs with a focus on material and structural approaches toward enhancement in mechanical stress durability.

The performance of TFTs is degraded further by repeated cycles of mechanical bending. Jeong et al. [54] reported that the use of stress-absorbing organic layers can extend the functionality of TFTs by minimizing electrical degradation. For flexible solar cell applications, Sibinski and Znajdek [55] and Zardetto et al. [56] provided some details about the issues with TCOs and how mechanical strain affects the stability of the TCO layer and the resultant cell efficiency. Additionally, Alkhazali et al. [57] have evaluated the mechanical and electrical properties of PEDOT and ITO thin films; their results showed that PEDOT has better integrity when subjected to strain compared to ITO. Other works on aluminum and molybdenum films by Hamasha et al. [58] and Alkhazali et al. [59] showed the important role of film thickness in resisting crack formation, where thicker films were more resistant and suffered electrical degradation. These cumulated results highlight the fact that material selection, thickness optimization, and substrate compatibility are crucial factors in enhancing the mechanical reliability of flexible electronics. The presented body of research will go toward developing more robust flexible devices, a contribution that goes well with the sustainable development goals in the advancement of technology and durability within the electronic domain.

In this respect, particular interest is given to $CrSi_2$ thin films due to their properties, such as high thermal and chemical stability, good electrical conductivity, and the possibility of obtaining these properties on flexible substrates-for instance, PET. $CrSi_2$ is a semi-metallic material; as such, it represents a strong candidate for flexible electronics, where required electrical performance has to be stable under mechanical stress. Unlike most other conductive materials, $CrSi_2$ exhibits its conductive properties within a wide range of environmental conditions, something rather important for flexible electronics, which may face changes in temperature, humidity, and other external factors.

$CrSi_2$ films, when deposited onto flexible substrates, automatically become subjected to the mechanical strains accompanying substrate deformation. Of these stresses, those due to repeated or sustained strain are able to initiate and propagate microcracks in the film. The formation of microcracks corresponds to mechanical limits in the material and often is initiated at grain boundaries, surface imperfections, or other points of weakness where stress is concentrated. As these cracks propagate, they eventually disrupt the pathways of conduction in the film and result in increased resistance. The latter is gradual degradation, with partial loss of conductivity as the widening and deepening of cracks happen-or even sudden in nature, at which point a critical point might be reached where the structural integrity of the film utterly fails.

The crack formation and propagation in $CrSi_2$ thin films will, therefore, have a direct impact on their electrical performance because even minor interruptions in the conductive network may strongly increase the resistance [60]. In extreme conditions, when cracks completely go through the film, it may cause total conductivity loss and the electronic device may cease to work. This susceptibility to mechanical strain creates a critical issue for the application of $CrSi_2$ films in flexible electronics, where electrical connectivity has to be preserved during deformation. Thus, the investigation into the behavior that the $CrSi_2$ films exhibit under applied strain, especially concerning crack initiation and propagation characteristics, becomes very vital in understanding their mechanical limits.

The study of the crack formation mechanism and the involved factors that affect the growth of cracks has thrown light on the durability and resilience of the $CrSi_2$ films in flexible applications. The knowledge gained might be useful in the optimization of the design, deposition process, and thickness of $CrSi_2$ films to enhance performance and longevity against mechanical stress. This will all facilitate the failure modes in such films for enhanced predictability and further mitigation, hence contributing to the development of more reliable and durable flexible electronics capable of operating effectively under extreme conditions. Present work hence provides valuable data on the mechanical and electrical behavior of CrSi2 thin films highly essential in their potential use in next-generation flexible and stretchable electronic devices.

In this work, we report the electrical and mechanical response of $CrSi_2$ thin films, sputtered onto PET substrates, for two values of thickness (100 nm and 200 nm). We will report the resistance change with the Percentage Change of Electrical Resistance (PCER), where resistance variation is monitored during progressive straining until total electrical disconnection is reached. It addresses the relationship between the strain, PCER, and

crack formation in detail, which can be used to provide further insight into how film thickness affects fracture mechanics and electrical degradation. This work will support the quantification of the $CrSi_2$ thin films' structural limitations during mechanical loading and will be an important contribution towards resistant, flexible electronic materials.

2. Materials and Methods

The mechanical and electrical properties of several $CrSi_2$ thin films sputtered on PET substrates were investigated in the present study through structured experimental procedures. In the first step, PET substrates were prepared by cutting uniformly sized 10 mm × 100 mm pieces from a 127-µm-thin PET sheet obtained from Plasma Quest, using a precision tool to avoid any variation among the samples. Cleaned PET substrates were subsequently introduced into a sputtering chamber equipped with a $CrSi_2$ target where RF magnetron sputtering would be carried out under strictly controlled conditions. The setup used was provided by Beijing Technol Science Co., Ltd., using $CrSi_2$ targets from MSE Supplies. The vacuum chamber was evacuated to below 2.5 × 10^-3 Pa, and Argon gas flowed at 29 sccm with an RF power setting of 250 W. Substrates were rotated at 20 rpm in order to provide a uniform deposition. Samples in the first batch were coated for one hour, yielding a 100 nm thick $CrSi_2$ layer , and samples in the second group were coated with a $CrSi_2$ layer, which is 200 nm thick after two hours of deposition. The film thickness was in situ monitored by QCM measuring the frequency change of a vibrating quartz crystal due to the accumulation of material on it. This frequency shift is proportional to the thickness of the film and usually used with sputtering devices to ensure accurate film depositions.

Tensile testing of the $CrSi_2$-coated PET samples was carried out following deposition. Each sample was mounted in an Instron tensile testing machine with an 80 mm gauge length. To quantify electrical resistance during testing, copper tape contacts applied 10 mm from each end of the film were connected to an NI myDAQ ohmmeter from National Instruments. This enabled continuous logging of the resistance data every second for analysis.

Tensile tests were performed at 1 mm/s; four samples for each thickness, that is, 100 nm and 200 nm, were stretched to failure to make sure of the reliability and repeatability of the results obtained. Moreover, a subset of samples was stretched to specified strains of 7.5%, 10%, and 12.5% of the gauge length and then examined by a JEOL Ltd. scanning electron microscope (SEM). With SEM, in situ observations of strain-induced cracks, deformation, and morphological changes were conducted on $CrSi_2$-coated surfaces to elucidate the mechanisms of sputtered film failure. The schematic of the testing set-up that includes the tensile tester, electrical resistance measurement, and post-deformation SEM imaging is below.

The change in electrical resistance due to mechanical strain was quantified by the common metric given by Equation 1. PCER may be defined as:

$$\text{PCER} = \frac{(\text{R} - \text{Ro})}{\text{Ro}} \times o - Ro \qquad (1)$$

where R represents the initial resistance, allowed a normal comparison in the change of resistance from one sample to another independent of the geometry and initial resistance of samples. This metric is particularly useful for assessing the strain-resistance relationship in brittle thin films like $CrSi_2$.

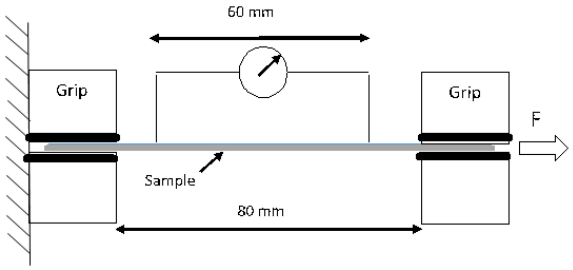

Figure 1. Schematic illustration of the specimen and grips.

3. Results and Discussion

While previous studies have explored the mechanical and electrical behavior of various conductive thin films on flexible substrates, limited attention has been given to semiconducting materials like chromium disilicide ($CrSi_2$), particularly in terms of their fracture behavior under uniaxial tensile strain. Most existing work has focused on materials such as ITO, AZO, and PEDOT, with relatively few investigations into the crack initiation, propagation, and corresponding electrical degradation in $CrSi_2$ films. Furthermore, the influence of film thickness on failure modes and strain tolerance in $CrSi_2$ systems remains underexplored. This gap hinders the ability to design $CrSi_2$-based flexible electronic components with optimized mechanical durability. The present study addresses this shortcoming by providing a systematic analysis of crack development and electrical performance in $CrSi_2$ thin films of two distinct thicknesses, offering new perspectives for material selection and structural design in flexible electronics.

Figure 2 presents SEM images of as-deposited $CrSi_2$ thin films on PET substrates for thickness of 100 nm on the left and 200 nm on the right. The given images confirm the surface morphology of $CrSi_2$ films deposited by sputtering under identical conditions and only varied by deposition time to achieve the said thicknesses. With this in mind, it is expected that the surface morphology would be similar on these two thicknesses, as indeed observed. This homogeneity in that respect shows that, regardless of the thickness, the same structural arrangement is produced in $CrSi_2$ thin films when this deposition method is used. Figure 2 therefore gives an idea of the typical surface morphology of $CrSi_2$ thin films obtained under controlled sputtering conditions and henceforth stands as a baseline for further property analysis.

Figure 3: SEM images of a 100 nm thick $CrSi_2$ thin film deposited on a PET substrate after stretching to 7.5% of the original length. The image highlights clearly the direction of the applied load with a yellow double-headed arrow pointing horizontally across the image. Moreover, enlarged fractions of the image show a close-up view of minute cracks that develop due to the applied strain. It can be observed that such cracks propagate in the direction perpendicular to the line of action of the applied load, which is quite typical under conditions of tensile loading in materials. The small cracks in Fig. 3 start from the localized weak points in the $CrSi_2$ thin film, such as minor defects or grain boundaries, since the stress concentration

in case of tensile loading is larger. Under stretching, these concentrations of stress exceed the local cohesive strength of the material, and crack growth begins. Such propagation could only be perpendicular to the direction of loading, in good agreement with fundamental mechanics, considering that brittle materials under tensile stress would bear maximum normal stress in directions perpendicular to the direction of the load. This orientation in stress encourages crack growth in the direction that relieves the applied tensile stress most effectively; hence, it is perpendicular to the load. The initiation and propagation of cracks within the $CrSi_2$ thin film on PET substrates are based on a combination of material brittleness, the flexibility of the substrate, and poor interfacial adhesion between the film and substrate. $CrSi_2$ has relatively brittle material that cannot absorb significant deformation energy before it fractures. With increasing applied strain, the film reaches a critical strain threshold beyond which it cannot support the load without fracturing. The PET substrate is flexible; however, due to the mismatch in mechanical properties between the two, it does not serve as an effective crack-arresting medium for cracks propagating in the $CrSi_2$ film.

Figure 4: SEM images of the $CrSi_2$ thin film with a thickness of 100 nm on a PET substrate subjected to a tensile strain of 10%. The image shows several cracks that have been labeled for viewing purposes as 1 through 7. At this higher strain, there is remarkably more crack growth than seen in Figure 3 at 7.5% strain. Cracks 1, 2, and 3 grow deeper appearing to penetrate the upper surface and possibly through the full thickness of the film. These cracks could still be connected at the interface to the $CrSi_2$ layer and the PET substrate and hence retain some continuity beneath the surface. Crack 7 is both wider and more pronounced, showing that it may extend through most of the film thickness, signaling significant material separation under strain. By contrast, cracks 4 and 5 are finer and do not fully penetrate the film, suggesting they have partially propagated due to the applied tensile stress. At 7.5% strain (Figure 3), the cracks were finer and more localized, with no evidence of complete film penetration. With increased strain to 10%, the density and severity of cracks continued to increase, with many of the cracks apparently penetrating well into the interior of the film. This transition from partial cracks at 7.5% to potentially fully penetrating cracks at 10% suggests a threshold behavior wherein strain beyond some critical level leads rapidly to deterioration in the structural integrity of the film and toward more extensive and interconnected cracking.

This increase to 10% strain amplifies the localized stress concentrations at points of weakness in the $CrSi_2$ film, thus favoring the initiation and growth of cracks. For tensile stress, the film will experience maximum normal stress along the direction perpendicular to the load, with any pre-existing cracks spreading and advancing further. It is possible that such a transition, from fully penetrating to finer cracks, might relate to the local variability of material properties, film thickness uniformity, and adhesion across the film-substrate interface. With increased strain, weak areas of the film reach their fracture limits earlier, eventually resulting in variability in crack depth and continuity.

This figure clearly emphasizes the critical role of strain level in influencing crack development and propagation in $CrSi_2$ thin films and provides substantial knowledge regarding the mechanical limits in a film and fracture behavior under tensile stress.

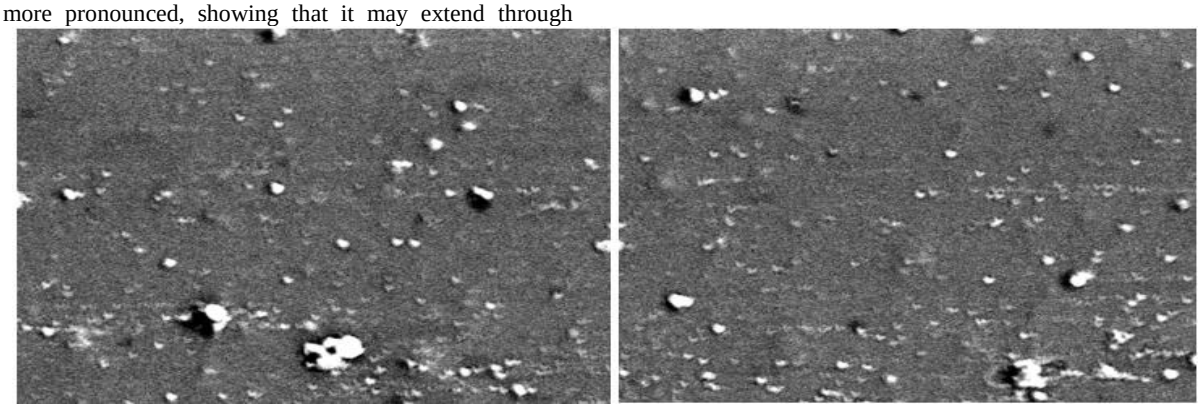

Figure 2. As deposited $CrSi_2$ Thin Films on PET; 100 nm (left), 200 nm (right)

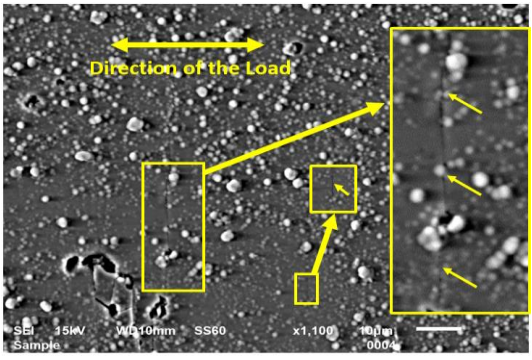

Figure 3. SEM image showing crack development in 100 nm $CrSi_2$ film stretched to X% strain.

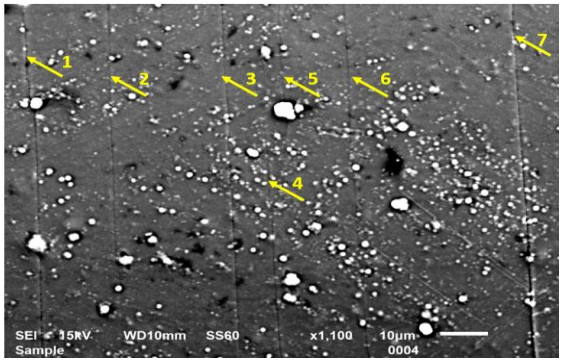

Figure 4. Cracks in a 100 nm Thick Film Stretching to 10% of the Original Length.

Figure 5: SEM images of 100 nm thick $CrSi_2$ on PET substrates at 12.5% tensile strain. As compared to the cracks in Figures 3 and 4 corresponding to 7.5% and 10% strains, respectively, the cracks here are appearing wider and deeper. Significantly at 12.5% strain, there is no obvious increase in the population of cracks, but the opening of the cracks has considerably increased, reflecting further growth and increased separation within the same crack network. In Figure 3, the cracks at 7.5% strain were very fine and localized, with most initiation as fine, shallow separations in the film. While by 10% strain in Figure 4, more cracks are present with deeper penetration; some fully cut through as well as partial, fine cracks. On the contrary, crack formation has gone to where additional cracks are minimal at 12.5% strain shown in Figure 5. Instead, the cracks that already existed opened up a lot, while the fracturing behavior of the film seemingly had transited from crack nucleation to crack propagation and widening. Where the strain is higher, for example 12.5%, the critical strain for crack nucleation has been exceeded; further deformation mainly widens and deepens pre-existing cracks. This behavior is consistent with brittle fracture mechanics, in which additional strain increases the stress concentration at the crack tips, promoting their growth rather than the formation of new cracks. Consequently, such a broadening of cracks with higher strain would be indicative of a reduced capability of the material to further support stretching, since the already present crack network undermines the structural integrity of the film. If this happens and the material is continually subjected to further strain, this could very well manifest into a situation of complete failure being realized eventually. Fig. 5 illustrates how fracture evolves with increasing tensile deformation in $CrSi_2$ thin films. In the present case, once a critical strain level is reached, further deformation promotes the growth of existing cracks to the creation of new ones. The resulting behavior clarifies the failure mechanism for $CrSi_2$ films on flexible substrates and helps define the limit of strain for practical applications.

Figures 6, 7 and 8 show SEM images for a 200 nm $CrSi_2$ film deposited on a PET substrate strained to 7.5%, 10% and 12.5%, respectively. These figures describe the progress of crack development for the 200 nm film as it undergoes increased tensile stress and can be compared with the cracking behavior seen in the 100 nm film at similar levels of strain.

In Figure 6, a strain of 7.5% is imposed on the 200 nm $CrSi_2$ film. Very few and very subtle cracks can be seen, and only a few fine cracks may appear across the surface. The majority of them are shallow with no noticeable width or depth to these cracks at this stage, which could be viewed as an initial response to the tensile stress that the film undergoes. It is believed that the thicker 200 nm film is able to support initial strain with minimal fracture at this strain level, since only limited development of cracks was observed, as increased thickness provides enhanced resistance to crack initiation compared to the 100 nm film at the same strain level.

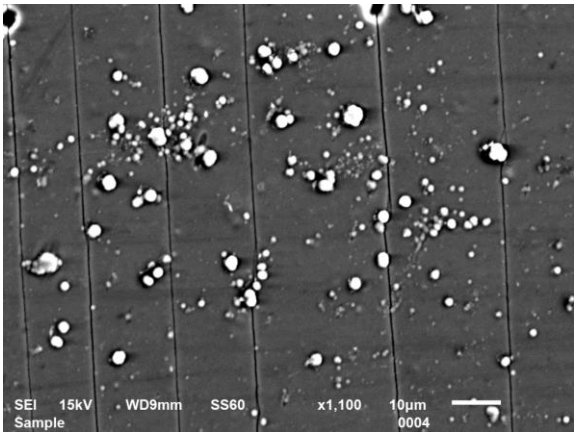

Figure 5. Cracks in a 100 nm Thick Film Stretching to 12.5% of the Original Length.

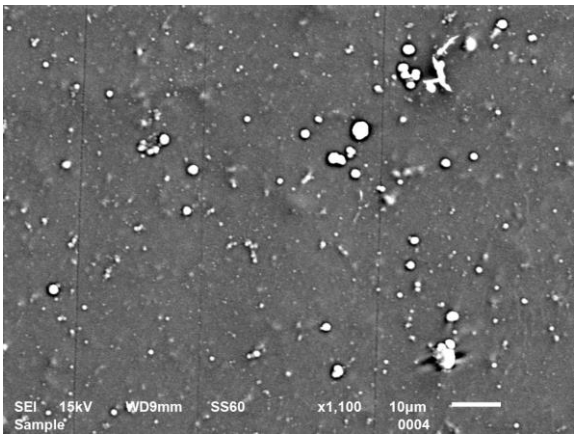

Figure 6. Cracks in a 200 nm Thick Film Stretching to 7.5% of the Original Length.

Figure 7 presents the stretched film to 10% of its original length. More cracks are visible at this level of strain; they are much more evident and wider than at 7.5% strain. These cracks propagate deeper through the film at a thickness of 200 nm, demonstrating that the film now cannot impede significant crack growth with increased stress. Although more pronounced compared to 7.5% strain, the cracks are not yet as extensive or numerous as for the 100 nm film under the same conditions. This again indicates that the added thickness of the 200 nm film allows for greater tolerance against tensile forces, delaying extensive crack formation.

In Figure 8, the film has been stretched to 12.5% strain. At this strain level, the cracks are significantly wider, deeper, and more spread across the surface when compared to the cracks in the 100-nm film at a similar strain level. For the case of the 200-nm film, however, the cracks remain relatively more spaced apart and fewer additional cracks have formed compared to the 100-nm film. While cracks propagating in the thicker film indeed seem to propagate in a much more stable, less chaotic fashion, this is most likely due to the greater film thickness, which has dispersed the applied stress much more evenly, along with providing resistance to fracture across a broader area.

Whereas comparable films of 100-nm thickness showed retardation in crack growth initiation and propagation, the latter has shown the same when compared to 200-nm thick films. This can be understood from the increased thickness providing more material through

which applied stress can be absorbed and distributed while reducing the local stress concentration at weak points. In contrast, the 100 nm thick film is much thinner and reaches its fracture limit much faster; therefore, under the same strain conditions, crack initiation and propagation will occur more rapidly. The increased resistance to crack formation in the thicker film and more stable propagation of cracks at higher levels of applied strain bring into focus how film thickness can be employed as a means of tailoring the fracture mechanics of materials such as $CrSi_2$ for flexible applications where tensile resilience is desired.

Figure 9 PCER as a function of the strain of 100 nm thick $CrSi_2$ thin films RF-sputtered on PET substrates. For this data, four samples were stretched and curves for maximum, mean, and minimum PCER have been presented. The data trends up to a strain level just below 0.025 beyond which complete electrical disconnection occurs across all samples. The figure is truncated at this point because the trend of PCER needs to be focused on, without including the data for disconnection.

For all samples, the steep rise in PCER is consistent with very little variation from each other as strain increases. Such similarity among the samples infers uniformity in behavior due to the electrical response of $CrSi_2$ thin films under tensile stress. The values of PCER have remained close enough to show a common trend in resistance increase with the progression of strain. First, for small strains, PCER is relatively close to zero, reflecting stable resistance. However, when strain reaches about 0.01, PCER starts growing extensively, following an exponential-like growth up to the cut-off point near 0.025.

Such a raise of PCER is intimately related to the formation and growth of cracks in $CrSi_2$ films. Indeed, when the level of strain is low, the structure of the film remains pretty much intact, which brings minimal change in resistance. With the increase in strain, first micro-cracks develop and propagate, more precisely perpendicular to the applied load, leading to larger disruption of the conductive paths of the film. This is further increased, with micro-cracks that are grown, causing progressive disconnections of the conductive network of the film. The resistance increases rapidly. This leads to the sharp rise in PCER. This increase is consistent with the crack development observed in SEM images, where the width and number of cracks are seen to increase as strain approaches 0.025. This type of damage eventually leads to a complete loss of electrical continuity at strains between 0.025 and 0.03, which explains the disconnection observed in all samples beyond this range.

While Figure 9 is representative data that shows the average PCER of multiple 100 nm samples with little spread, Figure 10 shows the large variability between the 200 nm samples as higher strain is applied and the films begin to electrically disconnect. This again points out that film thickness plays a role in consistency and cracking under strain, as represented by the differences between Figures 9 and 10.

Indeed, each sample in Figure 10 shows its specific features in the PCER response with increasing strain and therefore differs in structural response to increased strain and likely delamination behavior. Sample 1 becomes electrically disconnected at a strain below 0.1, while it has a rather smooth PCER curve. This would imply that Sample 1 fractured progressively without major delamination, hence enabling a more stable rise in resistance up to complete electrical failure. Sample 2 disconnected prior to reaching 0.1 strain yet exhibits a lot of fluctuation in PCER beyond 0.08 strain. The up-and-down variations are indicative that parts of the film might have delaminated from the substrate and caused intermittent contact and disconnection within the conductive network. This would indicate that, upon stretching, parts of the film were detaching, partially attaching again, and finally losing contact entirely, hence explaining the irregular trend in the PCER curve.

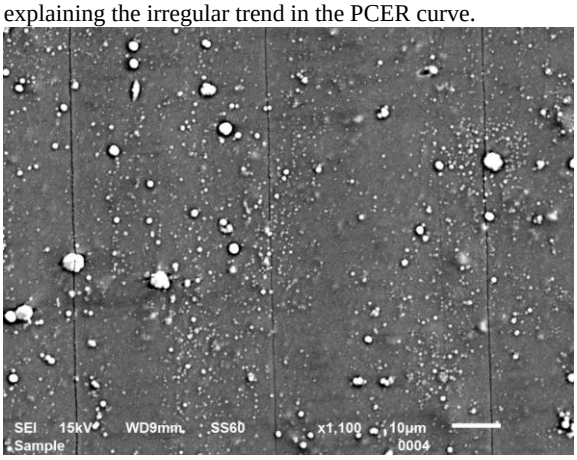

Figure 7. Cracks in a 200 nm Thick Film Stretching to 10% of the Original Length.

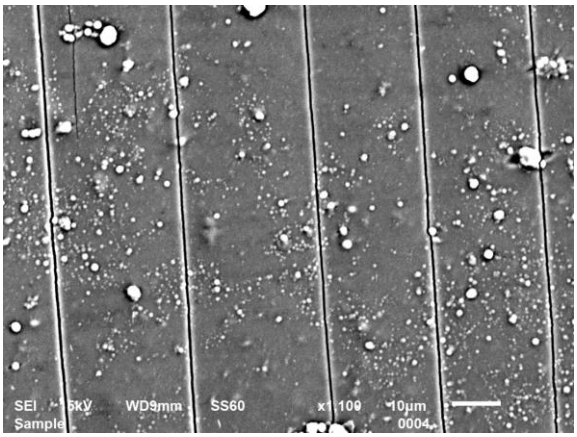

Figure 8. Cracks in a 200 nm Thick Film Stretching to 12.5% of the Original Length.

Sample 3 does not detach until at a strain of ~0.1625, and its PCER curve has no deviation, which means the crack propagation is stable with no delamination occurring. Lack of fluctuations indicates good adhesion of this sample to the substrate, which enabled a smooth increase in resistance with strain until complete disconnection. Sample 4 reaches the highest values of PCER before disconnection, showing steep increases of PCER. The steep increase and high amplitude of PCER indicate that Sample 4 probably sustained the conductive path for the longest time under increasing strain while cracks developed gradually before complete failure.

This variability in the behavior of the 200 nm samples can be explained by the scientific differences in film adhesion and uniformity of structure, along with the effect that thickness would have on crack propagation. The 200 nm thickness allows for greater accumulated stress and,

therefore, delayed disconnection compared to the films of 100 nm thickness seen in Figure 9, where trends in PCER were more uniform and disconnection occurred at lower levels of strain. Larger volume films have more significant crack propagation dynamics and are also more susceptible to delamination under tensile strain.

Compare this with Figure 9, in which the 100 nm films exhibited a more uniform trend in PCER with less scatter between samples. The reason for this uniformity is the smaller material thickness that restricts the complicated cracking and delamination. In the thinner films, cracks propagate more uniformly, leading to similar PCER increases across samples and faster disconnection. For the 200 nm films in Figure 10, the extra thickness can support larger internal stress gradients in the film; promoting diverse failure mechanisms such as delamination, as in Sample 2, and delayed cracking, as in Samples 3 and 4.

Figure 10 is indicative of a more complex relationship between film thickness and the propagation of cracks through film with regard to electrical resistance under strain. Specifically, cracks are forming and propagating in thicker films that may result in partial or intermittent contact within the conductive paths, which is manifested as fluctuations in PCER in samples exhibiting delamination. Indeed, thicker films can retain higher capability of strain resistance at the beginning, but it is more varied in failure mechanism with the increase of strain. In this way, film thickness is an important consideration when designing flexible electronics that need to have consistent performance under stress.

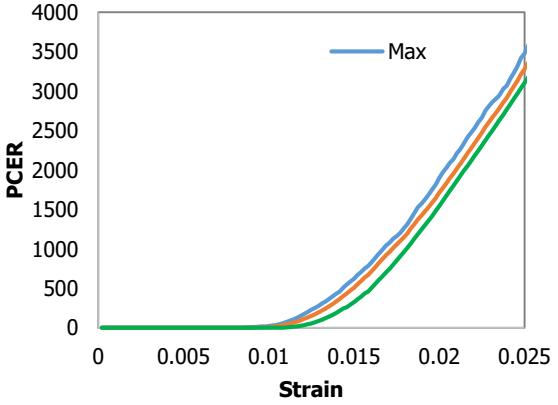

Figure 9. PCER vs. Strain for 100 nm $CrSi_2$ Thin Films on PET Substrates

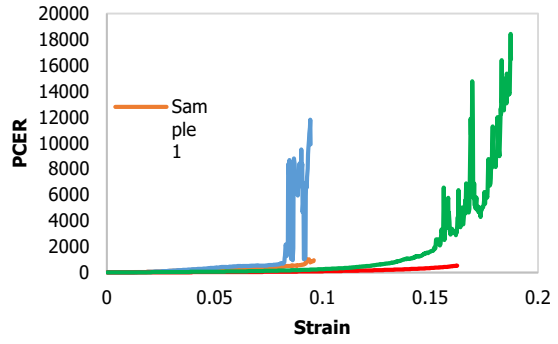

Figure 10. PCER vs. Strain for 200 nm $CrSi_2$ Thin Films on PET Substrates

4. Conclusions

In the present work, mechanical and electrical properties of $CrSi_2$ films on PET substrates subjected to tensile strains were systematically investigated with particular emphasis on the development of cracks and their ensuing impact on electrical degradation. The experiments performed in this work highlight the crucial role of thickness in $CrSi_2$ films toward strain tolerance and resistance to electrical disconnection. While the 100 nm films are functional at low strain, crack propagation occurs rapidly with significant increases in resistance that accelerate electrical failure. In contrast, 200 nm thick films exhibit increased mechanical durability; onset of cracking is delayed and the rise in resistance is more gradual, likely from the mitigation of stresses over the thicker film.

These results illustrate the progressive development of cracks in $CrSi_2$ films subjected to tensile stress, growing from micro-cracks at low strain to fully penetrating fractures at higher strain levels. The film thickness is a driving force for such nucleation-dominated versus extensive propagation of cracks, where thicker films can distribute stress more uniformly and delay catastrophic failure. Also, variability in the PCER trends of the 200 nm samples emphasizes a role of thickness in the mitigation of these strain-induced failure mechanisms like delamination and partial electrical disconnection.

These results therefore underscore a very important thickness optimization opportunity for $CrSi_2$ thin films in the field of flexible electronics, where mechanical robustness and consistent electrical performance are of essence. The findings from this research provide the necessary insight into the study of fracture mechanics and electrical degradation patterns in these films, which will be useful in designing robust flexible electronic components capable of withstanding tensile stress without failure. Other factors could also form the basis of further work: environmental influences and substrate-film interface modifications can be the pathways to enhance strain tolerance in $CrSi_2$ films for applications.

References

[1] A. K. Ababneh, A. S. Hijazin, and A. M. Jawarneh, "A novelty for thermal energy storage utilizing the principle of solid to solid phase change in a lithium sulfate at elevated temperatures." *Solar Energy*, Vol. 163, 2018, 45–53.

[2] A. M. Jawarneh, M. Al-Tarawneh, M. K. Ababneh, and H. Tlilan, "Solar energy availability on horizontal and tilted surfaces: A case study." *International Review of Mechanical Engineering*, Vol. 6, No. 4, 2012, 901–917.

[3] A. K. Ababneh, A. M. Jawarneh, H. M. Tlilan, and M. K. Ababneh, "The effects of the secondary fluid temperature on the energy transfer in an unsteady ejector with a radial-flow diffuser." *Heat and Mass Transfer*, Vol. 46, No. 1, 2009, 95–105.

[4] A. M. Jawarneh, A. Al-Shyyab, H. Tlilan, and A. Ababneh, "Enhancement of a cylindrical separator efficiency by using double vortex generators." *Energy Conversion and Management*, Vol. 50, No. 6, 2009, 1625–1633.

[5] H. Imai, J. Akita, and H. Niizawa, "Incentives for Technology Development and Project Based Mechanisms: Case of Renewable Energy Project." *Jordan Journal of Mechanical and Industrial Engineering*, Vol. 4, No. 1, 2010.

[6] T. K. Ibrahim, J. Thaddaeus, C. A. Popoola, I. Iliyasu, and A. A. Alabi, "Improvement of Wear Rate Properties of a Brown Pumice and Coal Ash Particulates Reinforced Aluminum Composite for Automobile Brake Manufacturing, Through Optimization and Modelling." *Jordan Journal of Mechanical and Industrial Engineering*, Vol. 18, No. 4, 2024.

[7] A. M. Jawarneh, F. M. Al-Oqla, and A. Abu Jadoo, "Transient behavior of non-toxic natural and hybrid multi-layer desiccant composite materials for water extraction from atmospheric air." *Environmental Science and Pollution Research*, Vol. 28, No. 33, 2021, 45609–45618.

[8] S. Odeh, S. Nijmeh, and B. Akash, "Performance evaluation of solar-assisted double-tube evaporator heat pump system." *International Communications in Heat and Mass Transfer*, Vol. 31, No. 2, 2004, 191–201.

[9] Corzo, D.; G. Tostado-Blázquez; D. Baran. Flexible electronics: Status, challenges and opportunities. *Frontiers in Electronics*, 2020. 1. 594003.

[10] Wang, X.; Z. Liu; T. Zhang. Flexible sensing electronics for wearable/attachable health monitoring. *Small*, 2017. 13. (1): 1602790.

[11] Huang, S.; Y. Liu; Y. Zhao; Z. Ren; C.F. Guo. Flexible electronics: Stretchable electrodes and their future. *Advanced Functional Materials*, 2019. 29. (6): 1805924.

[12] Alzoubi, K.; M.M. Hamasha; S. Lu; B. Sammakia. Bending fatigue study of sputtered ITO on flexible substrate. *Journal of Display Technology*, 2011. 7. (11): 593–600.

[13] Rim, Y.S.; S.-H. Bae; H. Chen; N. De Marco; Y. Yang. Recent progress in materials and devices toward printable and flexible sensors. *Advanced Materials*, 2016. 28. (22): 4415–4440.

[14] Hamasha, M.M.; K. Alzoubi; S. Lu; S.B. Desu. Durability study on sputtered indium tin oxide thin film on polyethylene terephthalate substrate. *Thin Solid Films*, 2011. 519. (18): 6033–6038.

[15] Khan, S.; S. Ali; A. Bermak. Recent developments in printing flexible and wearable sensing electronics for healthcare applications. *Sensors*, 2019. 19. (5): 1230.

[16] Keum, K.; J.W. Kim; S.Y. Hong; J.G. Son; S.-S. Lee; J.S. Ha. Flexible/stretchable supercapacitors with novel functionality for wearable electronics. *Advanced Materials*, 2020. 32. (35): 2002180.

[17] Zhang, D.; T. Huang; L. Duan. Emerging self-emissive technologies for flexible displays. *Advanced Materials*, 2020. 32. (15): 1902391.

[18] Li, L.; Z. Lou; D. Chen; K. Jiang; W. Han; G. Shen. Recent advances in flexible/stretchable supercapacitors for wearable electronics. *Small*, 2018. 14. (12): 1702829.

[19] Wu, Y.; Y. Ma; H. Zheng; S. Ramakrishna. Piezoelectric materials for flexible and wearable electronics: A review. *Materials & Design*, 2021. 211: 110164.

[20] Hassan, M.; G. Abbas; N. Li; A. Afzal; Z. Haider; S. Ahmed; X. Xu; C. Pan; Z. Peng. Significance of flexible substrates for wearable and implantable devices: Recent advances and perspectives. *Advanced Materials Technologies*, 2022. 7. (4): 2100773.

[21] Sun, B.; Y.-Z. Long; Z.-J. Chen; S.-L. Liu; H.-D. Zhang; J.-C. Zhang; W.-P. Han. Recent advances in flexible and stretchable electronic devices via electrospinning. *Journal of Materials Chemistry C*, 2014. 2. (7): 1209–1219.

[22] Harris, K.D.; A.L. Elias; H.-J. Chung. Flexible electronics under strain: A review of mechanical characterization and durability enhancement strategies. *Journal of Materials Science*, 2016. 51. (6): 2771–2805.

[23] Wu, W. Stretchable electronics: Functional materials, fabrication strategies and applications. *Science and Technology of Advanced Materials*, 2019. 20. (1): 187–224.

[24] Hamasha, M.M.; K. Alzoubi; S. Lu. Behavior of sputtered indium–tin–oxide thin film on polyethylene terephthalate substrate under stretching. *Journal of Display Technology*, 2011. 7. (8): 426–433.

[25] Burtch, N.C.; J. Heinen; T.D. Bennett; D. Dubbeldam; M.D. Allendorf. Mechanical properties in metal–organic frameworks: Emerging opportunities and challenges for device functionality and technological applications. *Advanced Materials*, 2018. 30. (23): 1704124.

[26] Peng, C.-Y.; M.M. Hamasha; D. VanHart; S. Lu; C.R. Westgate. Electrical and optical degradation studies on AZO thin films under cyclic bending conditions. *IEEE Transactions on Device and Materials Reliability*, 2012. 13. (2): 236–244.

[27] Zeng, W.; L. Shu; Q. Li; S. Chen; F. Wang; X.-M. Tao. Fiber-based wearable electronics: A review of materials, fabrication, devices, and applications. *Advanced Materials*, 2014. 26. (31): 5310–5336.

[28] Wong, W.S.; A. Salleo. *Flexible Electronics: Materials and Applications*. 2009: Springer Science & Business Media.

[29] Youssef, G. *Applied Mechanics of Polymers: Properties, Processing, and Behavior*. 2021: Elsevier.

[30] Yin, B.B.; W.K. Sun; X.Y. Zhang; K.M. Liew. Deciphering structural biological materials: Viewing from the mechanics perspective and their prospects. *Composites Part B: Engineering*, 2022. 245: 110213.

[31] Huang, H.; C. Dai; H. Shen; M. Gu; Y. Wang; J. Liu; L. Chen; L. Sun. Recent advances on the model, measurement technique, and application of single cell mechanics. *International Journal of Molecular Sciences*, 2020. 21. (17): 6248.

[32] Alexander, D.E. *Nature's Machines: An Introduction to Organismal Biomechanics*. 2017: Academic Press.

[33] Li, D.; W.-Y. Lai; Y.-Z. Zhang; W. Huang. Printable transparent conductive films for flexible electronics. *Advanced Materials*, 2018. 30. (12): 1704738.

[34] Cheng, T.; Y. Zhang; W.-Y. Lai; W. Huang. Stretchable thin-film electrodes for flexible electronics with high deformability and stretchability. *Advanced Materials*, 2015. 27. (22): 3349–3376.

[35] Naghdi, S.; K.Y. Rhee; D. Hui; S.J. Park. A review of conductive metal nanomaterials as conductive, transparent, and flexible coatings, thin films, and conductive fillers: Different deposition methods and applications. *Coatings*, 2018. 8. (8): 278.

[36] Zardetto, V.; T.M. Brown; A. Reale; A. Di Carlo. Substrates for flexible electronics: A practical investigation on the electrical, film flexibility, optical, temperature, and solvent resistance properties. *Journal of Polymer Science Part B: Polymer Physics*, 2011. 49. (9): 638–648.

[37] Alkhazali, A.S.; M.M. Hamasha; S. Lu; C.R. Westgate. A comparative study on electrical and mechanical behavior of indium tin oxide and poly(3,4-ethylenedioxythiophene) thin films under tensile loads. *IEEE Transactions on Device and Materials Reliability*, 2015. 15. (2): 174–180.

[38] Hamasha, M.M.; K. Alzoubi; J.C. Switzer; S. Lu; S.B. Desu; M. Poliks. A study on crack propagation and electrical resistance change of sputtered aluminum thin film on polyethylene terephthalate substrate under stretching. *Thin Solid Films*, 2011. 519. (23): 7918–7924.

[39] Alkhazali, A.; S. Hamasha; M.M. Hamasha; H. Khaled; R. Massadeh. Crack development and electrical degradation in chromium thin films under tensile stress on PET substrates. *Coatings*, 2024. 14. (11): 1403.

[40] Chate, G.R.; R.M. Kulkarni. Ceramic material coatings: Emerging future applications. *Advanced Ceramic Coatings for Emerging Applications*, 2023. 3.

[41] Hoffman, D.W.; J.A. Thornton. Internal stresses in sputtered chromium. *Thin Solid Films*, 1977. 40. (2): 355–363.

[42] Kawanabe, T.; J. Park; M. Naoe. Control of morphology and crystallinity of chromium sputtered film. *Materials Science and Engineering: A*, 1991. 134: 1305–1308.

[43] Lin, J.; J.J. Moore; W.D. Sproul; B. Mishra; Z. Wu. Modulated pulse power sputtered chromium coatings. *Thin Solid Films*, 2009. 518. (5): 1566–1570.

[44] Alkhazali, A.; M.M. Hamasha; H. Khaled; A. Alkhazaleh; M. Etier. Electro-mechanical properties of molybdenum thin film on polyethylene terephthalate subjected to tensile stress. *IEEE Transactions on Device and Materials Reliability*, 2024.

[45] Hamasha, M.M.; T.P. Dhakal; P. Vasekar; K. Alzoubi; S. Lu; D. Vanhart; C.R. Westgate. Reliability of sputter deposited aluminum-doped zinc oxide under harsh environmental conditions. *Solar Energy*, 2013. 89: 54–61.

[46] Zhang, Y.; Y. Yang; J. Zhao; R. Tan; W. Wang; P. Cui; W. Song. Optical and electrical properties of aluminum-doped zinc oxide nanoparticles. *Journal of Materials Science*, 2011. 46. (3): 774–780.

[47] Zhou, H.; D. Yi; Z. Yu; L. Xiao; J. Li. Preparation of aluminum doped zinc oxide films and the study of their microstructure, electrical and optical properties. *Thin Solid Films*, 2007. 515. (16): 6909–6914.

[48] Tahar, R.B.H. Structural and electrical properties of aluminum-doped zinc oxide films prepared by sol–gel process. *Journal of the European Ceramic Society*, 2005. 25. (15): 3301–3306.

[49] Wen, L.; B.B. Sahu; H.R. Kim; J.G. Han. Study on the electrical, optical, structural, and morphological properties of highly transparent and conductive AZO thin films prepared near room temperature. *Applied Surface Science*, 2019. 473: 649–656.

[50] Zeng, W.; Q. Li; S. Chen; F. Wang; X.-M. Tao. Fiber-based wearable electronics: Materials, fabrication, devices, and applications. *Advanced Materials*, 2014. 26. (31): 5310–5336.

[51] Sierros, K.A.; N.J. Morris; S.N. Kukureka; D.R. Cairns. Dry and wet sliding wear of ITO-coated PET components used in flexible optoelectronic applications. *Wear*, 2009. 267. (1-4): 625–631.

[52] Mohammed, D.W.; R.B. Ameen; J. Bowen; S.N. Kukureka. Twisting fatigue in multilayer films of Ag-alloy with indium tin oxide on PET for flexible devices. *Thin Solid Films*, 2018. 645: 241–252.

[53] Peng, C.-Y.; H. Sudarsanam; M.M. Hamasha; S. Lu; T.P. Dhakal; C.R. Westgate. Performance of aluminum-doped zinc oxide thin films under bending fatigue conditions. *Proceedings of IEEE Long Island Systems, Applications and Technology Conference*, 2012: 1–6.

[54] Zardetto, V.; T.M. Brown; A. Reale; A. Di Carlo. Substrates for flexible electronics: Electrical, flexibility, and solvent resistance properties. *Journal of Polymer Science Part B: Polymer Physics*, 2011. 49. (9): 638–648.

[55] Alkhazaili, A.; M.M. Hamasha; S. Lu; C.R. Westgate. Reliability of thin films: Mechanical behavior of ITO and PEDOT. *Microelectronics Reliability*, 2015. 55. (3-4): 538–546.

[56] Heremans, P.; A.K. Tripathi; E.C.P. Smits; B. Hou; G. Pourtois; G.H. Gelinck. Mechanical and electronic properties of TFTs on plastic. *Advanced Materials*, 2016. 28. (22): 4266–4282.

[57] Cheng, T.; Y. Zhang; W.-Y. Lai; W. Huang. Stretchable thin-film electrodes for flexible electronics. *Advanced Materials*, 2015. 27. (22): 3349–3376.

[58] Naghdi, S.; K.Y. Rhee; D. Hui; S.J. Park. Conductive nanomaterials as transparent coatings. *Coatings*, 2018. 8. (8): 278.

[59] Yin, J.; P. Hu; J. Luo; L. Wang; M.F. Cohen; C.-J. Zhong. Nanoparticle assembly for flexible devices. *ACS Nano*, 2011. 5. (8): 6516–6526.

[60] Han, K.-L.; H.-J. Jeong; K.-S. Jeong; S. Oh; J.-S. Park. Mechanical durability of oxide thin-film transistors on flexible substrates. *Journal of Physics D: Applied Physics*, 2019. 52. (48): 483002.